Author Manuscript

Author Manuscript

Author Manuscript

Author Manuscript

HHS Public Access

Author manuscript

Mol Pharm. Author manuscript; available in PMC 2016 May 04.

Published in final edited form as:

Mol Pharm. 2015 May 4; 12(5): 1356–1365. doi:10.1021/mp500589c.

Rapid and Persistent Delivery of Antigen by Lymph Node Targeting PRINT Nanoparticle Vaccine Carrier To Promote Humoral Immunity

Sarah N. Mueller[†], **Shaomin Tian**[‡,§], and **Joseph M. DeSimone**[*,†,§,∥,⊥,#]

[†]Department of Chemistry, University of North Carolina at Chapel Hill, Chapel Hill, North Carolina 27599, United States

[‡]Department of Microbiology & Immunology, University of North Carolina at Chapel Hill, Chapel Hill, North Carolina 27599, United States

[§]Lineberger Comprehensive Cancer Center, University of North Carolina at Chapel Hill, Chapel Hill, North Carolina 27599, United States

[∥]Institute for Nanomedicine, University of North Carolina at Chapel Hill, Chapel Hill, North Carolina 27599, United States

[#]Department of Chemical and Biomolecular Engineering, North Carolina State University, Raleigh, North Carolina 27695, United States

[⊥]Sloan-Kettering Institute for Cancer Research, Memorial Sloan-Kettering Cancer Center, New York, New York 10021, United States

Abstract

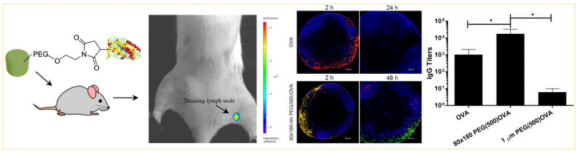

Nanoparticle delivery of subunit vaccines may increase vaccine efficacy, leading to a wide variety of safe and effective vaccines beyond those available through dosing inactivated or live, attenuated whole pathogens. Here we present a versatile vaccine delivery platform based on PRINT hydrogels made of biocompatible hydroxy-poly(ethylene glycol) (PEG) that is able to activate the complement system by the alternative pathway. These lymph node targeting

[*]**Corresponding Author** Department of Chemistry, University of North Carolina at Chapel Hill, CB#3290, 257 Caudill Laboratories, Chapel Hill, NC 27599-3290. Tel: (919) 962-2166. desimone@unc.edu..

Supporting Information Characterization and trafficking data for prescreened particles of various size and charge. This material is available free of charge via the Internet at http://pubs.acs.org.

The authors declare the following competing financial interest(s): The research reported in this paper received partial financial support from a venture capital-backed company that J. M. DeSimone cofounded, Liquidia Technologies (www.liquidia.com). Currently he has personal financial interests in Liquidia Technologies.

NOTE ADDED AFTER ASAP PUBLICATION This paper was published ASAP on April 8, 2015. The following additional information and ref 47 were added on April 14, 2015: Complement activation by PEG hydrogel nanoparticles may be dose and composition-dependent, as a recent study from our lab indicated that complement activation did not occur with low doses of hydrogel particles with different surface properties (Robbins et al., 2015).[47]

Author Manuscript Author Manuscript Author Manuscript Author Manuscript

nanoparticles (NPs) promote the immunogenicity of a model antigen, ovalbumin, showing comparable adjuvant effect to alum. We demonstrate that an antigen-specific humoral response is correlated with antigen delivery to the draining lymph nodes, in particular, B cell rich regions of the lymph nodes. 80 × 180 nm cylindrical NPs were able to sustain prolonged antigen presentation to antigen presenting cells (APCs) and elicit a stronger immune response than nondraining 1 × 1 μm NPs or rapidly clearing soluble antigen. The 80 × 180 nm NPs also show high levels of uptake by key APCs and efficiently stimulate $CD4^+$ helper T cell proliferation in vivo, further promoting antibody production. These features together produce a significant humoral immune response, superior to that produced by free antigen alone. The simplicity of the chemistries used in antigen conjugation to PRINT NPs confers versatility to this antigen delivery platform, allowing for potential application to many infectious diseases.

Keywords

particulate vaccine; *PRINT*; *lymphatic trafficking*; *PEGylation*

INTRODUCTION

Draining lymph nodes (LNs) are the primary site of action for initiating adaptive immunity, where T and B cells, major cell types involved in a humoral immune response, meet antigen or antigen-loaded antigen presenting cells (dendritic cells, macrophages).[1,2] To activate B cells and generate a robust humoral response, two signals are required: direct cross-linking of B cell receptors by antigens, and costimulatory signals from $CD4^+$ T cells (e.g., cytokines and CD40/CD40L binding).[3,4] Antigen presenting cells, especially dendritic cells (DCs), are critical in priming T cells to provide helper signals to B cells.[4–9] Because of the myriad activities of the immune system that take place in the lymph nodes, recent literature has focused on delivering vaccines directly to the draining LNs.[4,6,7,9,10] By targeting the draining LNs, vaccine uptake by antigen presenting cells (APCs), APC maturation, and antigen presentation to T and B cells may all occur in close proximity, thus increasing the potency of the resulting response.

Utilizing purified and synthetic pathogen subunits (peptides, polysaccharides, lipids, DNA, etc.) for vaccination has become an increasingly attractive option due to significantly improved safety profiles compared to whole pathogen-based vaccines. Subunit vaccines have gained significant clinical success in some diseases, e.g., HPV vaccines (Gardasil from Merck and Co., Cervarix from GlaxoSmithKline), seasonal influenza vaccines, pneumococcus, HBV, diphtheria, pertussis, etc. However, there is still a tremendous need for new strategies to improve subunit vaccines and expand their application to a wider variety of diseases. Since purified pathogen subunits used in subunit vaccines are usually poor immunogens, experiencing nonspecific degradation and metabolism in vivo and subject to rapid clearance from the body,[10–13] different strategies are used to improve the immunogenicity of these subunit antigens such as the addition of adjuvants or incorporation into different vaccine delivery vehicles. Particle mediated delivery has shown great potential for subunit vaccine development and has gained increasing attention.[6,10–12,14–23] Size, shape, and surface properties of particle vectors can be manipulated in order to target key

Author Manuscript Author Manuscript Author Manuscript Author Manuscript

APCs and promote cell uptake of antigens via phagocytosis, or facilitate self-drainage and direct delivery of vaccine components to lymph node-resident immune cells.[10–13,24] Surface display of antigens on particle carriers may allow multivalent interaction with B cells, mimicking presentation by natural pathogens and enabling more efficient cross-linking of cognate B cell receptors, thereby increasing potency of these agents[10,17,25] and achieving dose sparing effects.[14,25]

Many parameters of particulate vaccine carriers (charge, size, and surface properties) may all contribute to the quality of the resulting immune response. Previous work on the effects of lymphatic trafficking and efficacy of particulate vaccines has explored delivery vehicles such as liposomes, polymeric particles, and albumin hitchhiking molecules, among others.[2,16,19,20,23,26,27] There is a narrow particle size range that appears to harness lymphatic flow to the lymph node without becoming trapped at the site of injection; however, within the range of 20–100 nm NPs, the optimal particle size appears to be widely system dependent.[19,21,28,29]

Herein we present a versatile vaccine delivery platform based on hydrogel particles made of hydroxy-poly(ethylene glycol) (PEG), fabricated via PRINT technology (particle replication in nonwetting templates),[30–32] a unique mold-based particle fabrication process. The highly tunable nature of PRINT allows for a great degree of control over NP size, aspect ratio, charge, and surface functionality, facilitating a systematic study of these effects on NP trafficking through the lymphatic system and the subsequent immune response. We establish that this vaccine carrier has the capacity to deliver subunit vaccine components to the draining LNs in a sustained manner and elicit a significant antigen-specific humoral immune response.

MATERIALS AND METHODS

Materials

DyLight 680 maleimide and maleimide-PEG(500)-NHS were purchased from Thermo Fisher Scientific, Inc. Alexa Fluor 488 maleimide was purchased from Invivogen. Maleimide-PEG(5k)-NHS and NHSPEG(260)-OH were purchased from Creative PEGworks. EndoGrade Ovalbumin (98% purity, <1 EU/mg) was purchased in bulk from Hyglos GmbH and tested periodically for endotoxin contamination. Alexa Fluor 555 conjugated ovalbumin was purchased from Life Technologies. Tetraethylene glycol monoacrylate (HP(250)A) was synthesized in house. PRINT molds were supplied by Liquidia Technologies. All other chemicals and reagents were obtained from Sigma-Aldrich, Inc., unless otherwise noted.

Animals

Female Balb/c, C57BL/6, and OT-II mice were purchased from Jackson Laboratory and used at age 6–12 weeks. All experiments involving the mice were carried out in accordance with an animal use protocol approved by the University of North Carolina Animal Care and Use Committee.

Author Manuscript Author Manuscript Author Manuscript Author Manuscript

Fabrication of Hydrogel NPs via the PRINT Process

The fabrication of nano- and micron-sized NPs was achieved by mold-based PRINT particle fabrication technology[31–33] using a composition shown in Table S1 in the Supporting Information. Briefly, cure-site monomer (CSM) solutions were prepared at 2.5 wt % solids in dry methanol. NPs used in trafficking studies included 2 wt % of a fluorescent dye, either DyLight 680 maleimide or AlexaFluor 488 maleimide, covalently cross-linked into the particle matrix. The film-split technique for preparing NPs was performed as described in the following: using a #5 Mayer rod, 350 μL of CSM solution was cast on a sheet of corona treated poly(ethylene terephthalate) (PET), followed by brief evaporation of solvent with a heat gun to yield a transparent film (delivery sheet). Patterned Fluorocur PRINT molds (Liquidia Technologies) were laminated against the delivery sheet with moderate pressure (40 psi) and delaminated at the same pressure. The filled mold was laminated against corona-treated PET and subsequently cured in a UV-LED chamber (Phoseon, λmax =395 nm) for 3.5 min under a nitrogen environment. After photocuring, the mold was removed to reveal an array of NPs on PET. NPs were mechanically harvested off the PET with sterile water (1 mL/40 $in.^2$). NPs were washed via centrifugation (30 min, 14,000 rpm, 4 °C), removal of supernatant, and resuspension in fresh, sterile solvent. NP yield was determined by thermogravimetric analysis (Q5000IR, TA Instruments). To conjugate ovalbumin (OVA) to the NPs, particles were first PEGylated with heterobifunctional PEG, maleimide-PEG(5k)-NHS, or maleimide-PEG(500)-NHS, by reacting 1 mg of NPs with 1.6 μmol of PEG plus triethylamine (100 μL) in DMF at a final concentration of 1 mg of NPs in 1.4 mL.[33] The reaction was run at room temperature overnight with shaking at 1400 rpm. NPs were then washed with fresh DMF. Residual amine groups on the surface of NPs were quenched with 13.5 μmol of NHSPEG(260)-OH (Creative PEGworks) following the same PEGylation procedure above, or with 150 μmol of succinic anhydride, reacted in the presence of 186 μmol of pyridine for 30 min with agitation at 1400 rpm. NPs were then washed into water. OVA was conjugated to the free maleimide groups by reacting NPs and OVA in a 1:1 weight ratio at a NP concentration of 4 mg/mL in borate buffer pH 9.5 with 0.1 wt % PVOH, MW 2 kDa, overnight at room temperature with shaking at 1400 rpm. NPs were washed with buffer to remove unbound protein and washed with water to remove residual salt. For PEG(0) NPs, OVA was conjugated to the NP surface by first reacting the free amines on the NPs with succinic anhydride as used in quenching above, followed by reaction with OVA, EDC (1-ethyl-3-(3-(dimethylamino)propyl)-carbodiimide), and sulfo-NHS according to protocol by Thermo Scientific. NPs were washed with buffer to remove unbound protein and washed thoroughly with water to remove residual salt. Antigen conjugation levels were controlled based on the ratio of NP:OVA during the conjugation reaction, varying from 1:1 to 4:1, with a constant total volume of 1 mL for each reaction.

NP Characterization

Scanning electron microscopy (SEM) enabled imaging of hydrogel NPs that were dispersed on a silicon wafer, dehydrated, and coated with approximately 1.5 nm of Au/Pd (Hitachi S-4700, FEI Helios Nanolab 600). Size and ζ-potential measurements were conducted on ~20 μg/mL NP dispersions in water using a Zetasizer Nano ZS particle analyzer (Malvern Instruments Inc.). OVA conjugation was measured using a standard BCA Assay (Fisher).

Author Manuscript Author Manuscript Author Manuscript Author Manuscript

Lymphatic Drainage Studies

Mice were dosed with 50 μg of fluorescent NPs in 20 μL of isotonic solution, subcutaneously in the rear right footpad. To monitor OVA drainage, 5 μg of OVA labeled with AlexaFluor 555 (Sigma), soluble or conjugated to NPs, was injected into the footpad. Mice were sacrificed at the indicated time points, and draining popliteal LNs (PLNs) from both the dosed and contralateral control sides were resected. Resected PLNs were imaged for total fluorescence and/or homogenized into a single cell suspension for analysis of NP distribution in various cell types by flow cytometry. Additional dosed PLNs were frozen at −80 °C in OCT medium (TissueTek) for histological analysis. The percent-injected dose was calculated as (mass of NPs in PLN) ÷ (50 μg injected dose) × 100. Mass of NPs in PLN was calculated as (fluorescence of dosed PLN) − (fluorescence of control PLN) and compared to a standard curve of NPs. No NP fluorescence was found in other lymph nodes or major organs (liver, kidney, spleen, lung, heart) at any time point.

Ex Vivo Imaging

Imaging of resected LNs was done using an IVIS-Lumina II (PerkinElmer, Inc. Hopkinton, MA) with analysis done on Living Image software, version 3.2 (PerkinElmer, Inc. Hopkinton, MA). For optimal performance of the DyLight 680 dye, excitation and emission filters were set to 675 and 720 nm, respectively.

Flow Cytometry

Draining LNs were resected at indicated time points postsubcutaneous injections of 50 μg of dye-labeled NPs. Single cell suspensions of LNs were made physically with frosted slides. Cells were stained with CD11c-eFluor450, F4/80-FITC, B220-PE, and PDCA-PerCP-eFluor710, all from eBioscience. Cells were then examined with Cyan ADP (Dako) and analyzed with Summit software. For DC subset analysis, LN cells were stained with CD11c-eFluor450, CD8-FITC, and DEC205-PE (eBioscience).

In Vivo $CD4^+$ T Cell Proliferation

$CD4^+$ T cells recognizing OVA323–339 were isolated from spleens of OT-II transgenic mice with a kit (Miltenyi Biotech). The purified T cells were labeled with 4 μM CFSE fluorescent dye for 10 min at 37 °C, and 10 million cells were adoptively transferred into each C57BL/6 mouse intravenously. On the next day, mice were subcutaneously immunized with 1 μg of OVA, soluble or NP-loaded. Spleens were harvested 4 days later, and single cell suspensions were stained with CD4-PE-Cy7 and Valpha2-eFluor450 (eBioscience). Cells were then examined with Cyan ADP (Dako) and analyzed with Summit software.

Complement Activation

A C3a sandwich ELISA was performed to measure complement activation in mouse serum following incubation with NPs. EIA plates (Corning 9018) were coated with an anti-mouse C3a monoclonal antibody (BD Biosciences, clone I87-1162) diluted 1:250 in coating buffer (eBioscience) overnight at 4 °C. Mouse serum was incubated 1:1 with either PBS or NPs at 37 °C for 50 min. Serial dilutions of purified mouse C3a protein (BD Biosciences) were included in each ELISA plate to establish a standard curve. Serum samples were added to

Author Manuscript Author Manuscript Author Manuscript Author Manuscript

wells in duplicate (50 μL total volume) and incubated for 3 h. Anti-C3a-biotinylated detection antibody (BD Biosciences, clone I87-419) was used at a 1:500 dilution in 1× assay diluent, and incubated for 40 min. Streptavidin-HRP (BD) was diluted 1:250 in 1× assay diluent for 30 min. 1× TMB substrate solution (eBioscience) was added to develop color. The reaction was stopped with 0.2 N H_2SO_4, and absorbance was read at 450 nm with a reference wavelength of 570 nm on a SpectraMax (Molecular Devices) plate reader.

Confocal Microscopy

Resected draining LNs were frozen in OCT medium without fixation. 10 μm sections were made with Leica cryostat, fixed with ice cold acetone, and stained with purified anti-B220 (eBioscience) coupled with goat anti-rat IgG-Alexa Fluor 488 or -Alexa Fluor 647 (Invitrogen), anti-B220-biotin (eBioscience) coupled with Streptavidin-Alexa Fluor 555 (Invitrogen), or CD11c-biotin (eBioscience) coupled with Streptavidin-Alexa Fluor 633 (Invitrogen). Sections were examined with a Zeiss 710 confocal microscope.

Immunizations and Antibody ELISA

C57BL/6 mice, 6–8 weeks old, were immunized with soluble OVA or NP-conjugated OVA at 5 μg per mouse, subcutaneously in the flank. Mice were primed on day zero and boosted on day 21. Plasma samples were collected by bleeding mice submandibularly on day 28, and OVA-specific antibody production was examined by ELISA. Briefly, EIA plates (Corning) were coated with 10 μg/mL OVA in ELISA coating buffer (eBioscience) at 4 °C overnight. The wells were washed and blocked with 200 μL per well of 3% BSA in PBST (PBS with 0.05% Tween 20) for 2 h. Plasma samples were diluted in blocking buffer and incubated for 2 h. The wells were washed extensively with PBST, and anti-OVA IgG was detected using HRP conjugated goat anti-mouse IgG (Invitrogen) and was visualized by adding 100 μL of TMB (eBioscience) to each well. The reaction was stopped after 11 min with 50 μL of 0.2 M H_2SO_4. Optical densities (OD) were read at 450 and 570 nm. The antibody titer was determined as the highest dilutions with OD (450–570 nm) > 0.1.

RESULTS AND DISCUSSION

Nanoparticle delivery of protein subunit vaccines to the lymph nodes allows antigens to interact directly with the immune system. Additionally, surface display of protein antigens similar to antigen presentation by natural pathogens may boost therapeutic efficacy of these subunits to the levels associated with whole pathogen vaccines with an improved safety profile.[4,8,34] This study aimed to evaluate PRINT nanoparticles (NPs) of various size, aspect ratio, and surface characteristics for their ability to traffic through the lymphatic system and to explore the use of these NPs for antigen delivery in vaccine applications.

A delivery vector that traffics quickly and efficiently to the draining lymph nodes would be beneficial for delivering antigens to B cells and other antigen presenting cells (APCs) resident in the lymph nodes. A panel of rod/cylindrical PRINT NPs of different size, aspect ratio, and surface charge (Table S2 in the Supporting Information) were injected subcutaneously in mice to screen for the ability to drain to the popliteal lymph nodes (PLNs) (Figure 1). While NPs larger than 100 nm in size do not traditionally drain well through the

Author Manuscript Author Manuscript Author Manuscript Author Manuscript

lymphatics system as shown in the literature,[19,21,28,29] rod shaped NPs with two dimensions under 100 nm may be sufficiently small to traffic through the extracellular matrix of the lymphatic system in order to drain to the lymph nodes while maintaining benefits over traditional spherical NPs in terms of cellular uptake as well as an increased surface area for cargo loading.[31] Ex vivo imaging of resected PLNs revealed that, within 2 h of injection, anionic 80 × 180 nm rod NPs were visible in the PLN, with a time dependent accumulation over 48 h. In contrast, all other NPs, regardless of size and charge, generally remained at the site of injection with less than 0.2% (0.1 μg NPs) of the injected dose trafficking to the PLN. In terms of trafficking abilities, NP surface charge appears to be the most important determinant when selecting a self-draining NP delivery vehicle, followed by NP size. Anionic 80 × 180 nm NPs, the best self-draining particle type of the particles surveyed, were chosen for further vaccine delivery studies.

Surface display of antigens greatly increases the chances of direct antigen presentation to B cells, facilitating a more robust antibody response. To test immunogenicity of antigen delivered by the hydrogel NP carrier, a model protein antigen ovalbumin (OVA) was covalently conjugated to the surface of 80 × 180 nm NPs through multiple chemistries, including poly(ethylene glycol) (PEG)-based linkers, a common bioconjugation technique used to control the distance between ligands and NPs. PEGylation is frequently used to increase circulation half-life of small molecule drugs, biologics, and nanoparticles by decreasing the binding of serum proteins and opsonins, thus decreasing recognition by the mononuclear phagocyte system (MPS).[34] For vaccine carriers, PEGylation may enhance drainage of NPs from the site of injection to the lymph nodes by blocking interactions with the extracellular matrix (ECM); however, a high level PEGylation, especially with high molecular weight PEG, could be undesirable as it may prevent NP uptake by phagocytic APCs.[6] In order to examine the effect of PEG linker length on lymphatic drainage and cell uptake, the model antigen OVA was conjugated to the surface of NPs via 5000 Da molecular weight PEG (PEG(5k)), 500 Da molecular weight PEG (PEG(500)), or a direct amide bond from protein to NP (PEG(0)) representing long, medium, and short linkers, respectively. After conjugation of antigen, all NPs remained very well dispersed with polydispersity index (PDI) below 0.15 (Table 1). Antigen conjugation levels varied based on the ratio of NP:OVA during the conjugation reaction. 48 h postinjection, significantly more PEG(500)OVA NPs reached PLNs as compared to the PEG(5k)OVA and PEG(0)OVA NPs (Figure 2a). Surface modification with the long PEG(5k) linker was apparently not favorable for lymphatic drainage. Further comparison with bare NPs and no-OVA PEG(500) NPs indicated that the increase in trafficking for the PEG(500)OVA NPs came from the synergy between PEG(500) and OVA, rather than either component alone. PEGylation with a dense layer of short PEG(500) may stabilize the NPs under physiological conditions and decrease interactions with the ECM, while longer PEG(5k) may have a greater chance of becoming entangled with the biopolymers in the ECM.[6,35] Additionally, compared to 80 × 180 nm PEG(500)OVA NPs, the 1 μm PEG(500)OVA NPs showed poor lymphatic trafficking on par with the bare 1 μm NPs (Figures 1 and 2a); conjugation with PEG linker and OVA did not improve the drainage of 1 μm NPs. These results demonstrate that, with particles of similar surface charge, the size of NP is an essential determinant for lymphatic drainage

Author Manuscript Author Manuscript Author Manuscript Author Manuscript

patterns of particle vectors, which can be subsequently modulated by different lengths of PEG linkers.

The best draining particles, 80 × 180 nm PEG(500)OVA NPs, also showed rapid drainage to the lymph node and were present in the PLN in as little as 5 min after injection, with the concentration of NPs in the PLN continuously increasing over 48 h (Figure 2b). At 48 h, NP trafficking reached 10% of total injected dose (5 μg of NPs), five times higher than bare anionic 80 × 180 nm NPs (2%, 1 μg, Figure 1).

In order to elicit an immune response, the NP delivery vector must be able to ensure that the antigen arrives at the site of action without being degraded or released prematurely. To investigate the drainage of NP bound OVA compared to that of free OVA and confirm that OVA was still bound to the NPs when they arrived at the LNs, we tagged the NPs and OVA with two different fluorophores. Free OVA (red) drained rapidly and was observed in the PLN 2 h after injection, but was no longer detectable at 24 h (Figure 2c). This is consistent with literature indicating that soluble proteins are subject to quick lymphatic clearance.[13] For 80 × 180 nm PEG(500)OVA NPs, particles and OVA (shown in yellow as overlapping of green NPs and red OVA) also drained quickly, as seen previously with the trafficking experiments, and were colocalized in the subcapsular regions of the PLN 2 h after injection. NP-OVA (yellow) stayed in the PLN much longer than soluble OVA (red) and was still observed at 48 h after injection (Figure 2c), although the quantity of NP-OVA (yellow) versus NPs alone (green) decreased over time. Importantly, OVA selectively accumulated in the B cell follicles, and the presence of OVA in this region persisted for up to 15 days. A similar phenomenon was also observed for 80 × 180 nm PEG(0)OVA (Figure 2c). This separation of antigen from the delivery vehicle is consistent with findings by Catron et al., who observed the cleavage of a model antigen from a particulate delivery vehicle upon trafficking to the lymph nodes.[36] They determined that this cleavage occurred in a protease-dependent manner over a course of several hours, allowing antigen to accumulate in B cell follicles without the need for the particles themselves to be taken up by APCs. Overall this result indicates that in general 80 × 180 nm hydrogel NPs are able to efficiently deliver antigen to B cells in the LNs, supporting sustained antigen retention in B cell rich regions. The longer residence time of NP-conjugated OVA in the PLN may help increase the interaction between antigen and B cells and LN-resident APCs compared to free OVA, resulting in an enhanced antibody response.

In addition to the delivery of antigens to B cells and cross-linking of cognate B cell receptors, eliciting a potent humoral response and B cell memory also requires help from $CD4^+$ T cells;[24] therefore good vaccine carriers need to be able to deliver antigens to APCs and prime T cells efficiently. Analysis of cells from draining LNs by flow cytometry showed that, 48 h postsubcutaneous dosing, 80 × 180 nm hydrogels with OVA linked through all three linker lengths reached 10–20% of the DCs, and 10–35% of the macrophages in the PLNs, while 1 μm PEG(500)OVA NPs were found in less than 2% of DCs or macrophages (Figure 3a), indicating that the 80 × 180 nm NPs may efficiently deliver antigens to key APCs. Although the total drainage to LNs of these three NPs with various linker lengths (Figure 2a) did not directly correlate with the uptake of NPs by cells in the PLNs, both results suggest that a long PEG linker is less favorable for antigen delivery to immune cells.

Author Manuscript Author Manuscript Author Manuscript Author Manuscript

The colocalization of the 80 × 180 nm PEG(500)OVA NPs with DCs was also observed by confocal microscopy analysis of sectioned draining LNs (Figure S1 in the Supporting Information), indicating that these NPs are able to access all regions of the PLNs where B cell and T cell activation can occur, facilitating activation of both humoral and cellular immune responses. While B cells did take up significantly more 80 × 180 nm PEG(500)OVA and 80 × 180 nm PEG(0)OVA NPs compared to the 80 × 180 nm PEG(5k) and 1 μm PEG(500)OVA NPs, less than 5% of B cells took up particles for all groups (Figure 3a). This is not surprising: B cells are not phagocytic cells, unlike macrophages and DCs, which are specialized for taking up particulate matter. Our own and others' work has shown that nonphagocytic cells like epithelial cells are much less efficient in internalizing neutral and negatively charged NPs.[37] However, anionic NPs can still be taken up efficiently through receptor-mediated endocytosis when a targeting ligand is available on NPs.[38] Activation of B cells requires recognition and uptake of antigens through their cognate B cell receptors. The accumulation of NPs in B cell regions would still greatly increase the chance of encountering an antigen by B cells carrying its cognate BCRs for initiation of an immune response. In addition, as seen in Figure 2c, over time proteases in the lymphatic fluid cleave antigen from the NPs, also allowing for the antigen to interact with B cells without the NPs being taken up.[36]

Lymph nodes are home to a large population of DCs, especially $CD8\alpha^+$ DCs, which have been shown to be the most efficient DCs in antigen cross-presentation.[6,9,39] In addition, there are other major DC subsets including migratory Langerhans cells and dermal DCs, normally resident in distal areas of the body, as well as LN resident double negative DCs as defined by surface markers CD8 and DEC205[22] (Figure S2 in the Supporting Information). Subsequent analysis of DCs from draining LNs showed that initially 80 × 180 nm PEG(500)OVA NPs distributed in all four different subsets of DCs somewhat evenly with an increase in the percentage of LN resident $CD8\alpha^+$ DCs over a 30 min period (Figure 3b). This suggests that these NPs are indeed self-draining, not fully dependent on uptake by migratory APCs to reach the LNs. This is further verified by the presence of NPs in the PLNs at as early as 5 min postinjection (Figure 3b): cell-mediated delivery of NPs has been shown to occur over several hours to days.[3,40] At 27 h after injection, the percentage of NP^+ LN resident DCs decreases and the percentage of NP^+ migratory dermal DCs increases, likely due to continuous uptake of NPs by dermal DCs at the injection site followed by cell mediated transport to PLNs. These results demonstrate that the 80 × 180 nm hydrogel NPs can traffic to the PLNs both through self-draining and through cell mediated delivery and are able to access various DC subsets, with a high percentage of $CD8\alpha^+$ DCs and dermal DCs internalizing NPs, potentially preparing them for T cell priming.

The T cell priming ability of the 80 × 180 nm PEG(500)OVA NPs was examined with an in vivo proliferation assay using $CD4^+$ OT-II cells that recognize peptide epitope $OVA_{323–339}$. As displayed in Figure 3c, immunizations with 80 × 180 nm PEG(500)OVA NPs loaded with just 1 μg of OVA effectively stimulated the proliferation of CFSE-labeled $CD4^+$ OT-II T cells, causing a dilution of the fluorescent dye. The dividing cells reached about 60% of total CFSE-labeled cells in 3 days (Figure 3d). On the other hand, minimum proliferation was seen in mice that were untreated or dosed with 1 μg of soluble OVA. Together with the flow cytometry data, we can deduce that the 80 × 180 nm PEG(500)OVA NPs are

Author Manuscript Author Manuscript Author Manuscript Author Manuscript

effectively taken up by APCs, where they can deliver antigen cargo and activate helper T cells.

The complement system not only acts as the first line of defense for the body but also links innate and adaptive immunity and plays an important role in peripheral lymph nodes to enhance B and T cell responses.[41] The complement system is activated by three different pathways: classical, lectin, and alternative; however, all three pathways share a common step: activating the central component C3. Hubbell and coworkers reported that nanoparticles can be engineered to activate the complement system and improve immune responses to vaccines.[16,42,43] Additionally, Link et al. showed that activation of complement played an important role in recognition of virus-like nanoparticles by noncognate B cells, leading to antigen retention by key DC subtypes.[44] Here we show that PRINT hydrogel NPs activate the complement system, as indicated by increase in the conversion of C3 to C3a (Figure 4a). Both bare and OVA-conjugated NPs promoted the conversion of C3 to C3a, suggesting that activation may result from the NP composition rather than postfabrication modifications to the NPs. However, surface modification with long chain PEG may reduce the capacity of the NPs to activate the complement system, possibly due to a higher degree of shielding of the NP surface groups that would otherwise interact with components in the complement system. Furthermore, EDTA but not EGTA blocked the conversion of C3 to C3a (Figure 4b), indicative of complement activation via the alternative pathway rather than the classical pathway. These results demonstrate that, in addition to the efficient LN targeted delivery of antigen, PRINT hydrogel NP vaccine vectors may potentially improve immune responses by activating the complement system.

Immunogenicity of antigen delivered by this NP vector was tested by vaccinating mice against OVA delivered either in soluble form or conjugated to NPs as described previously. The display of antigen on the NP surface may increase the chance of direct presentation of antigen to B cells, although this strategy may be less protective to the antigen than encapsulation techniques. The immune response to free versus particulate OVA was evaluated following a prime-boost regimen. Seven days after the boost dose, mice immunized with 80 × 180 nm PEG(500)OVA NPs showed a 10-fold increase in OVA-specific IgG production compared to free OVA and free OVA + bare NPs ($p < 0.05$, Figure 5a), whereas the NPs that were coinjected with free OVA did not augment the immune response. This data suggests that covalent conjugation to the NP vector is necessary for enhanced immunity. NP-OVA was compared to free OVA plus the adjuvant alum, the standard of care for adjuvanted vaccines.[45] Free OVA + alum elicited higher antibody titers than NP-OVA; however, NP-OVA + alum gave a significant increase in antibody response compared to free OVA + alum (Figure 5b), indicating that this NP-based vector for antigen delivery may be able to further improve the antibody response against protein antigen in adjuvanted vaccines. Previous work has shown that the PRINT hydrogel NPs induce no inflammatory response on their own;[46] therefore the major advantage of the NP vector over alum comes from its efficient delivery of antigen to immune system in addition to direct immunomodulation through complement activation.

The correlation between trafficking and immune response was examined by comparing the anti-OVA IgG antibody production after OVA delivery via 80 × 180 nm NPs with various

Author Manuscript Author Manuscript Author Manuscript Author Manuscript

PEG linker lengths as well as the 1 μm NPs. Interestingly, despite the influence PEG linker length had on NP trafficking (Figure 2a), PEG linker length appeared to have no statistical effect on antigen-specific IgG production (Figure 6a). All linker lengths showed a 10-fold increase in OVA-specific IgG production compared to free OVA, but the IgG levels were equivalent among the NP groups. However, the size of the NPs used to deliver OVA appeared to have a more dramatic effect on the total IgG. The antibody response against the 80 × 180 nm PEG(500)OVA NPs was over 1000 times higher than the response to the 1 μm PEG(500)OVA NPs ($p < 0.05$, Figure 6b). Remarkably, IgG response to 1 μm PEG(500)OVA NPs was even lower than that for soluble OVA, strongly suggesting that drainage of vaccine carrier and antigen interaction with LN-resident B cells are crucial to eliciting a humoral response. It is likely that there is a threshold amount of antigen needed in the lymph nodes for initiating a humoral immune response. This level may be sufficiently reached by the 80 × 180 nm NPs, including the relatively low self-draining 80 × 180 nm PEG(5k)OVA NPs, while the 1 μm NPs do not appear to deliver enough antigen to the LNs to do so.

CONCLUSION

In conclusion, we have designed and optimized a versatile vaccine delivery platform based on PRINT NPs. We demonstrate that the size, aspect ratio, charge, and surface characteristics of NPs are all important in improving the lymphatic trafficking of NPs and their subsequent uptake by key APCs. Anionic hydrogel NPs, with dimensions smaller than 100 nm, loaded with a model antigen showed high levels of self-drainage and were able to efficiently deliver antigen to B cells and major APCs, inducing antigen-specific humoral and cellular responses superior to free antigen alone. The simplicity of the chemistries used in antigen conjugation confers versatility to this delivery platform, allowing for potential application to many infectious diseases. Increasing the efficacy of subunit vaccines through a particulate delivery platform is of great interest and may lead to a wide variety of safe and effective vaccines based on dosing pathogen subunits.

Supplementary Material

Refer to Web version on PubMed Central for supplementary material.

ACKNOWLEDGMENTS

The authors thank Dr. Ashish Pandya for the synthesis of HP(250)A, the University of North Carolina Animal Studies Core for their assistance with animal experiments, and the Chapel Hill Analytical and Nanofabrication Laboratory (CHANL) for support with NP imaging. This work was supported by the NIH Director's Pioneer Award (5-DP1-CA174425-04) and Liquidia Technologies.

ABBREVIATIONS USED

NP	nanoparticle
PRINT	particle replication in nonwetting templates
APC	antigen presenting cell

Author Manuscript Author Manuscript Author Manuscript Author Manuscript

PLN	popliteal lymph node
LN	lymph node
DC	dendritic cell
OVA	ovalbumin

REFERENCES

(1). Moon JJ, Huang B, Irvine DJ. Engineering Nano- and Microparticles to Tune Immunity. Adv. Mater. 2012; 24:3724–3746. [PubMed: 22641380]

(2). Liu H, Moynihan KD, Zheng Y, Szeto GL, Li AV, Huang B, Van Egeren DS, Park C, Irvine DJ. Structure-Based Programming of Lymph-Node Targeting in Molecular Vaccines. Nature. 2014; 507:519–522. [PubMed: 24531764]

(3). Bachmann MF, Jennings GT. Vaccine Delivery: A Matter of Size, Geometry, Kinetics and Molecular Patterns. Nat. Rev. Immunol. 2010; 10:787–796. [PubMed: 20948547]

(4). Pal I, Ramsey JD. The Role of the Lymphatic System in Vaccine Trafficking and Immune Response. Adv. Drug Delivery Rev. 2011; 63(10–11):909–922.

(5). Belz G, Smith C, Bharadwaj M, Rice A, Jackson D. DCs as Targets for Vaccine Design. Cytotherapy. 2004; 6:88–98. [PubMed: 15203984]

(6). Hubbell JA, Thomas SN, Swartz MA. Materials Engineering for Immunomodulation. Nature. 2009; 462:449–460. [PubMed: 19940915]

(7). Cruz LJ, Tacken PJ, Rueda F, Domingo JC, Albericio F, Figdor CG. Targeting Nanoparticles to Dendritic Cells for Immunotherapy. Elsevier Inc (1st ed.). 2012; Vol. 509:143–163.

(8). De Temmerman M-L, Rejman J, Demeester J, Irvine DJ, Gander B, De Smedt SC. Particulate Vaccines: On the Quest for Optimal Delivery and Immune Response. Drug Discovery Today. 2011; 16:569–582. [PubMed: 21570475]

(9). Swartz MA, Hubbell JA, Reddy ST. Lymphatic Drainage Function and Its Immunological Implications: From Dendritic Cell Homing to Vaccine Design. Semin. Immunol. 2008; 20:147–156. [PubMed: 18201895]

(10). Ferreira SA, Gama FM, Vilanova M. Polymeric Nanogels as Vaccine Delivery Systems. Nanomedicine. 2013; 9:159–173. [PubMed: 22772049]

(11). Xiang SD, Scholzen A, Minigo G, David C, Apostolopoulos V, Mottram PL, Plebanski M. Pathogen Recognition and Development of Particulate Vaccines: Does Size Matter? Methods. 2006; 40:1–9. [PubMed: 16997708]

(12). Storni T, Kündig TM, Senti G, Johansen P. Immunity in Response to Particulate Antigen-Delivery Systems. Adv. Drug Delivery Rev. 2005; 57:333–355.

(13). Porter CJ, Charman SA. Lymphatic Transport of Proteins after Subcutaneous Administration. J. Pharm. Sci. 2000; 89:297–310. [PubMed: 10707011]

(14). Kasturi SP, Skountzou I, Albrecht RA, Koutsonanos D, Hua T, Nakaya HI, Ravindran R, Stewart S, Alam M, Kwissa M, Villinger F, Murthy N, Steel J, Jacob J, Hogan RJ, García-Sastre A, Compans R, Pulendran B. Programming the Magnitude and Persistence of Antibody Responses with Innate Immunity. Nature. 2011; 470:543–547. [PubMed: 21350488]

(15). Moon J, Suh H, Bershteyn A, Stephan M. Interbilayer-Crosslinked Multilamellar Vesicles as Synthetic Vaccines for Potent Humoral and Cellular Immune Responses. Nat. Mater. 2011; 10:243–251. [PubMed: 21336265]

(16). Reddy ST, van der Vlies AJ, Simeoni E, Angeli V, Randolph GJ, O'Neil CP, Lee LK, Swartz MA, Hubbell JA. Exploiting Lymphatic Transport and Complement Activation in Nanoparticle Vaccines. Nat. Biotechnol. 2007; 25:1159–1164. [PubMed: 17873867]

(17). Rice-Ficht AC, Arenas-Gamboa AM, Kahl-McDonagh MM, Ficht TA. Polymeric Particles in Vaccine Delivery. Curr. Opin. Microbiol. 2010; 13:106–112. [PubMed: 20079678]

Author Manuscript Author Manuscript Author Manuscript Author Manuscript

(18). John ALS, Chan CY, Staats HF, Leong KW, Abraham SN. Synthetic Mast-Cell Granules as Adjuvants to Promote and Polarize Immunity in Lymph Nodes. Nat. Mater. 2012; 11:1–8.

(19). Fifis T, Gamvrellis A, Crimeen-Irwin B, Pietersz GA, Li J, Mottram PL, McKenzie IFC, Plebanski M. Size-Dependent Immunogenicity: Therapeutic and Protective Properties of Nano-Vaccines against Tumors. J. Immunol. 2004; 173:3148–3154. [PubMed: 15322175]

(20). Zhuang Y, Ma Y, Wang C, Hai L, Yan C, Zhang Y, Liu F, Cai L. PEGylated Cationic Liposomes Robustly Augment Vaccine-Induced Immune Responses: Role of Lymphatic Trafficking and Biodistribution. J. Controlled Release. 2012; 159:135–142.

(21). Oussoren C, Storm G. Liposomes to Target the Lymphatics by Subcutaneous Administration. Adv. Drug Delivery Rev. 2001; 50:143–156.

(22). Zhan X, Tran KK, Shen H. Effect of the Poly(ethylene Glycol) (PEG) Density on the Access and Uptake of Particles by Antigen-Presenting Cells (APCs) after Subcutaneous Administration. Mol. Pharmaceutics. 2012; 9(12):3442–3451.

(23). Kaur R, Bramwell VW, Kirby DJ, Perrie Y. Manipulation of the Surface Pegylation in Combination with Reduced Vesicle Size of Cationic Liposomal Adjuvants Modifies Their Clearance Kinetics from the Injection Site, and the Rate and Type of T Cell Response. J. Controlled Release. 2012; 164:331–337.

(24). Johansen P, Mohanan D, Martínez-Gómez JM, Kündig TM, Gander B. Lympho-Geographical Concepts in Vaccine Delivery. J. Controlled Release. 2010; 148:56–62.

(25). Bershteyn A, Hanson MC, Crespo MP, Moon JJ, Li AV, Suh H, Irvine DJ. Robust IgG Responses to Nanograms of Antigen Using a Biomimetic Lipid-Coated Particle Vaccine. J. Controlled Release. 2012; 157:354–365.

(26). Al Kobiasi M, Chua BY, Tonkin D, Jackson DC, Mainwaring DE. Control of Size Dispersity of Chitosan Biopolymer Microparticles and Nanoparticles to Influence Vaccine Trafficking and Cell Uptake. J. Biomed. Mater. Res., Part A. 2012; 100:1859–1867.

(27). Moghimi SM. The Effect of Methoxy-PEG Chain Length and Molecular Architecture on Lymph Node Targeting of Immuno-PEG Liposomes. Biomaterials. 2006; 27:136–144. [PubMed: 16019063]

(28). Reddy ST, Berk DA, Jain RK, Swartz MA. A Sensitive in Vivo Model for Quantifying Interstitial Convective Transport of Injected Macromolecules and Nanoparticles. J. Appl. Physiol. 2006; 101:1162–1169. [PubMed: 16763103]

(29). Reddy ST, Rehor A, Schmoekel HG, Hubbell JA, Swartz MA. In Vivo Targeting of Dendritic Cells in Lymph Nodes with Poly(propylene Sulfide) Nanoparticles. J. Controlled Release. 2006; 112:26–34.

(30). Rolland JP, Maynor BW, Euliss LE, Exner AE, Denison GM, DeSimone JM. Direct Fabrication and Harvesting of Monodisperse, Shape-Specific Nanobiomaterials. J. Am. Chem. Soc. 2005; 127:10096–10100. [PubMed: 16011375]

(31). Gratton SEA, Ropp PA, Pohlhaus PD, Luft JC, Madden VJ, Napier ME, DeSimone JM. The Effect of Particle Design on Cellular Internalization Pathways. Proc. Natl. Acad. Sci. U.S.A. 2008; 105:11613–11618. [PubMed: 18697944]

(32). Gratton SEA, Williams SS, Napier ME, Pohlhaus PD, Zhou Z, Wiles KB, Maynor BW, Shen C, Olafsen T, Samulski ET, Desimone JM. The Pursuit of a Scalable Nanofabrication Platform for Use in Materials and Life Science Applications. Acc. Chem. Res. 2008; 41:1685–1695. [PubMed: 18720952]

(33). Perry JL, Reuter KG, Kai MP, Herlihy KP, Jones SW, Luft JC, Napier M, Bear JE, DeSimone JM. PEGylated PRINT Nanoparticles: The Impact of PEG Density on Protein Binding, Macrophage Association, Biodistribution, and Pharmacokinetics. Nano Lett. 2012; 12:5304–5310. [PubMed: 22920324]

(34). Wilson JT, Keller S, Manganiello MJ, Cheng C, Lee CC, Opara C, Convertine A, Stayton PS. pH-Responsive Nanoparticle Vaccines for Dual-Delivery of Antigens and Immunostimulatory Oligonucleotides. ACS Nano. 2013; 7(5):3912–3925. [PubMed: 23590591]

(35). Swartz MA. The Physiology of the Lymphatic System. Adv. Drug Delivery Rev. 2001; 50:3–20.

Author Manuscript Author Manuscript Author Manuscript Author Manuscript

(36). Catron DM, Pape KA, Fife BT, van Rooijen N, Jenkins MK. A Protease-Dependent Mechanism for Initiating T-Dependent B Cell Responses to Large Particulate Antigens. J. Immunol. 2010; 184:3609–3617. [PubMed: 20208013]

(37). Gratton SEA, Napier ME, Ropp PA, Tian S, DeSimone JM. Microfabricated Particles for Engineered Drug Therapies: Elucidation into the Mechanisms of Cellular Internalization of PRINT Particles. Pharm. Res. 2008; 25:2845–2852. [PubMed: 18592353]

(38). Wang J, Tian S, Petros RA, Napier ME, Desimone JM. The Complex Role of Multivalency in Nanoparticles Targeting the Transferrin Receptor for Cancer Therapies. J. Am. Chem. Soc. 2010; 132:11306–11313. [PubMed: 20698697]

(39). Wilson NS, El-Sukkari D, Belz GT, Smith CM, Steptoe RJ, Heath WR, Shortman K, Villadangos JA. Most Lymphoid Organ Dendritic Cell Types Are Phenotypically and Functionally Immature. Blood. 2003; 102:2187–2194. [PubMed: 12791652]

(40). Manolova V, Flace A, Bauer M, Schwarz K, Saudan P, Bachmann MF. Nanoparticles Target Distinct Dendritic Cell Populations according to Their Size. Eur. J. Immunol. 2008; 38:1404–1413. [PubMed: 18389478]

(41). Carroll MC. The Complement System in Regulation of Adaptive Immunity. Nat. Immunol. 2004; 5:981–986. [PubMed: 15454921]

(42). Thomas SN, van der Vlies AJ, O'Neil CP, Reddy ST, Yu SS, Giorgio TD, Swartz MA, Hubbell JA. Engineering Complement Activation on Polypropylene Sulfide Vaccine Nano-particles. iomaterials. 2011; 32:2194–2203.

(43). Fine DP, Marney SR, Colley DG, Sergent JS, Prez R. M. Des. C3 Shunt Activation in Human Serum Chelated with EGTA. J. Immunol. 1972; 109:807–809. [PubMed: 4627510]

(44). Link A, Zabel F, Schnetzler Y, Titz A, Brombacher F, Bachmann MF. Innate Immunity Mediates Follicular Transport of Particulate but Not Soluble Protein Antigen. J. Immunol. 2012; 188:3724–3733. [PubMed: 22427639]

(45). Baylor NW, Egan W, Richman P. Aluminum Salts in Vaccines—US Perspective. Vaccine. 2002; 20(Suppl. 3):S18–S23. [PubMed: 12184360]

(46). Roberts RA, Shen T, Allen IC, Hasan W, DeSimone JM, Ting JPY. Analysis of the Murine Immune Response to Pulmonary Delivery of Precisely Fabricated Nano- and Microscale Particles. PLoS One. 2013; 8:e62115. [PubMed: 23593509]

(47). Robbins GR, Roberts RA, Guo H, Reuter K, Shen T, Sempowski GD, McKinnon KP, Su L, DeSimone JM, Ting JPY. Analysis of human innate immune responses to PRINT fabricated nanoparticles with cross validation using a humanized mouse model. Nanomedicine. 2015; 11:589–599. [PubMed: 25596079]

Author Manuscript Author Manuscript Author Manuscript Author Manuscript

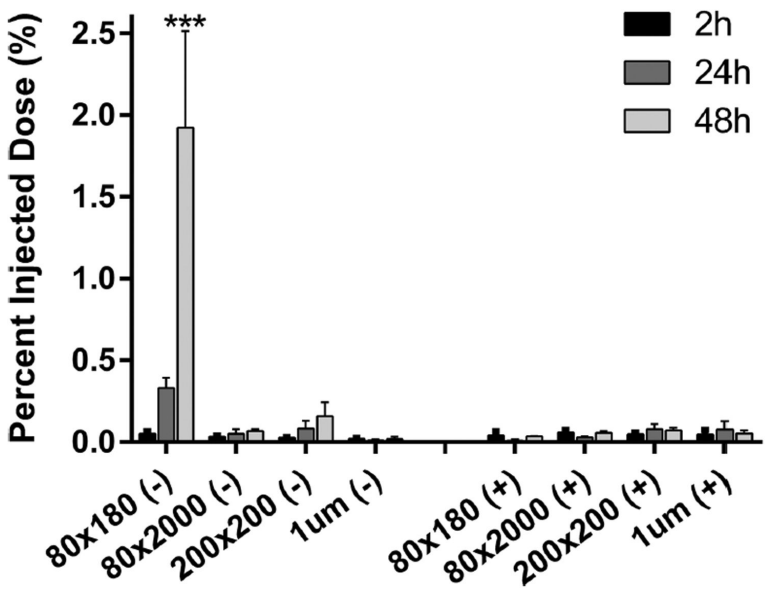

Figure 1.

Lymphatic drainage of blank hydrogel particles. Mice were injected with 50 μg of fluorescently labeled particles dispersed in 20 μL of isotonic solution in the hind footpad. Draining popliteal lymph nodes were resected and examined for particle fluorescence by IVIS imaging. Error bars stand for SEM, $N \geq 4$. Statistically significant differences between experimental groups were determined by two-way ANOVA followed by Tukey's multiple comparisons post-test. ***, $p < 0.001$.

Author Manuscript Author Manuscript Author Manuscript Author Manuscript

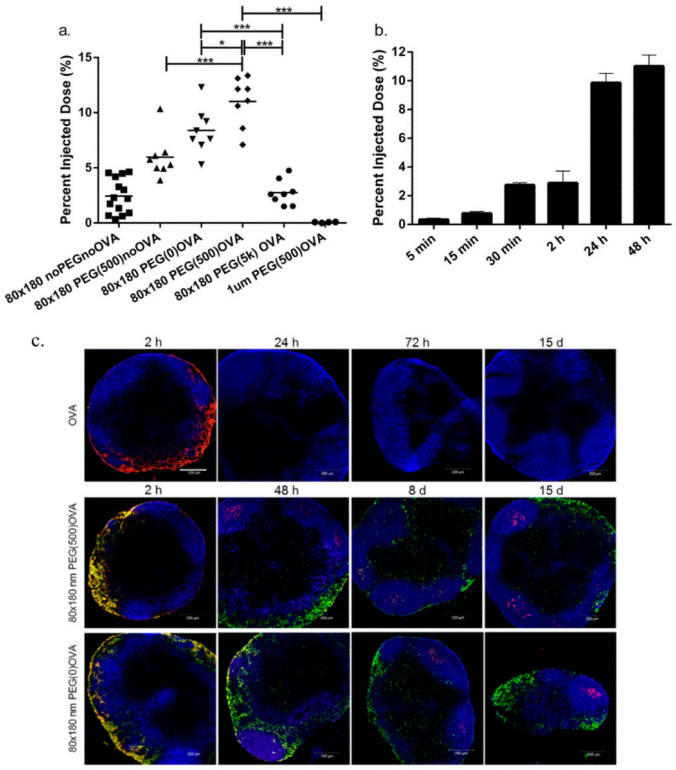

Figure 2.

Drainage of OVA-loaded hydrogel NPs to lymph nodes. (a) Total drainage of NPs in lymph nodes. 50 μg of fluorescently labeled 80 × 180 nm hydrogel NPs was subcutaneously injected into footpads of C57BL/6 mice, and draining popliteal LNs were collected at 48 h and imaged with IVIS Lumina. Mass of NPs administered was held constant with minor variations in OVA dosage. Statistically significant differences between experimental groups were determined by one-way ANOVA followed by Tukey's multiple comparisons test. *, $p < 0.05$; ***, $p < 0.001$. Error bars stand for SEM. $N = 4–14$. (b) 80 × 180 nm PEG(500)OVA NPs drained rapidly to the lymph nodes accumulated over 48 h. Error bars stand for SEM. $N = 4–8$. (c) Persistent delivery of antigen to B cells by hydrogels. Blue, B220 (B cells); green, NPs; red, OVA-AF555. Scale bar: 200 μm.

Author Manuscript Author Manuscript Author Manuscript Author Manuscript

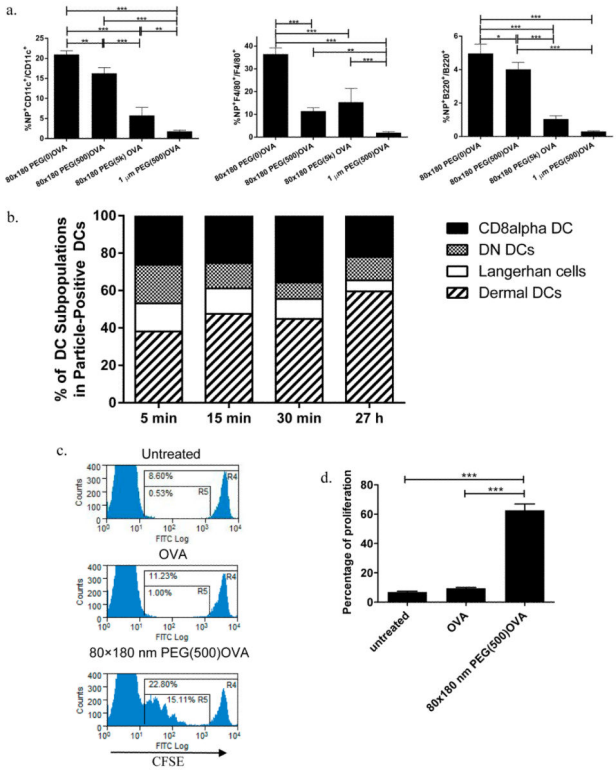

Figure 3.

Delivery of antigen to APCs and T cell priming by OVA-loaded hydrogel NPs. (a) 80 × 180 nm NPs are efficiently taken up by key antigen presenting cells (DCs, macrophages, and B cells respectively) in LNs 48 h postsubcutaneous injection, as analyzed by flow cytometry. $N \geq 4$. (b) Uptake of NPs by various DC subsets in draining LNs, with an increase in the percentage of migratory DCs over time. (c) In vivo $CD4^+$ OT-II T cell proliferation. (d) Quantitative analysis of OT-II T cell proliferation. The percentage of proliferation represents the ratio of cell numbers in R5 and R4 shown in panel c (R5/R4). N = 3–4. Hydrogel-mediated delivery of antigen is more efficient in stimulating $CD4^+$ T cell proliferation than soluble antigen. Statistically significant differences between experimental groups were determined by one-way ANOVA followed by Tukey's multiple comparisons test. Error bars stand for SEM. *, $p < 0.05$; **, $p < 0.01$, ***, $p < 0.001$.

Author Manuscript Author Manuscript Author Manuscript Author Manuscript

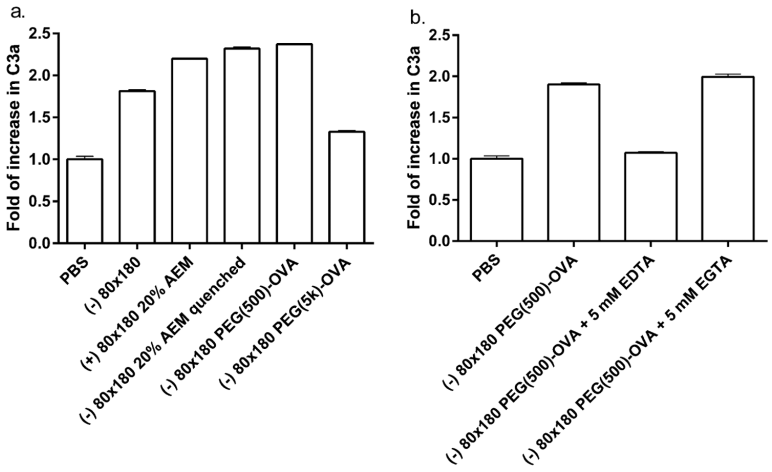

Figure 4.

Hydrogel NPs activate complement system. Serum from C57BL/6 mice was incubated with (a) 0.5 mg/mL NPs and (b) 1.2 mg/mL NPs for 50 min at 37 °C. Conversion from C3 to C3a was assayed by ELISA. The data represent one of two similar individual experiments; bars are average of two replicate wells in each experiment.

Author Manuscript Author Manuscript Author Manuscript Author Manuscript

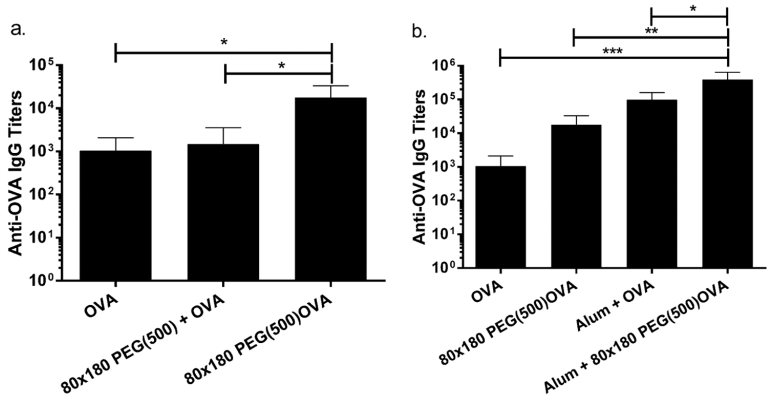

Figure 5.

NP conjugated OVA elicits higher antibody titers than soluble administration. (a) OVA conjugated to NPs elicits higher response than soluble OVA or soluble OVA admixed with NPs, indicating that conjugation to NPs is necessary for increased immunogenicity. (b) OVA delivered via NPs elicits higher antibody titers than soluble antigen when both groups are delivered with or without alum adjuvant. Mice were immunized on day 0 and again on day 21 with 5 μg of OVA, soluble or conjugated to PRINT hydrogel NPs. OVA-specific IgG in plasma was examined by ELISA. Statistically significant differences between experimental groups were determined by one-way ANOVA followed by Tukey's multiple comparisons test. *, $p < 0.05$; **, $p < 0.01$; ***, $p < 0.001$. Error bars stand for SEM. $N = 5$.

Author Manuscript Author Manuscript Author Manuscript Author Manuscript

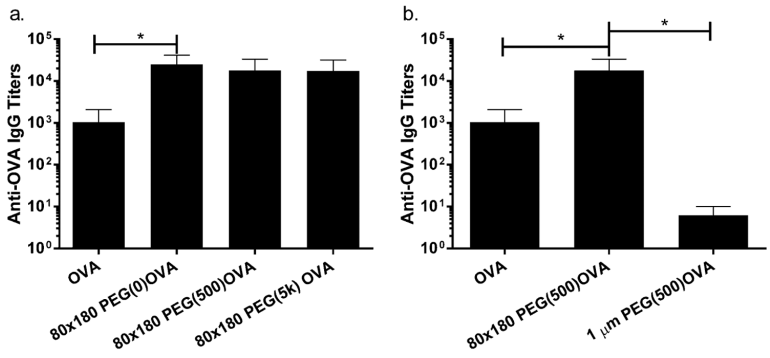

Figure 6.

Size rather than PEG linker length dramatically influences IgG response. (a) Length of PEG linker for OVA conjugation does not affect IgG response. (b) Large 1 μm NPs elicit lower IgG production than soluble administration or smaller 80 × 180 nm NPs. Mice were immunized as in Figure 5, and plasma IgG was evaluated by ELISA. Statistically significant differences between experimental groups were determined by one-way ANOVA followed by Tukey's multiple comparisons test. *, $p < 0.05$. Error bars stand for SEM. Data represent two or three individual experiments of $N = 4$.

Author Manuscript

Author Manuscript

Author Manuscript

Author Manuscript

Table 1

Characterization of OVA-Conjugated Particles

monomer	size (diam, nm)	PDI	zeta potential (mV)	OVA loading* (μg/mg NP)
80 × 180 nm bare	200.8 ± 11.6	0.025 ± 0.017	−24.6 ± 0.3	
80 × 180 nm PEG(0)OVA	246.8 ± 1.2	0.139 ± 0.010	−33.6 ± 1.2	54 ± 28
80 × 180 nm PEG(500)OVA	192.0 ± 2.1	0.044 ± 0.014	−39.3 ± 1.6	57 ± 24
80 × 180 nm PEG(5k)OVA	191.3 ± 0.6	0.076 ± 0.004	−27.5 ± 0.3	51 ± 36
1 μm PEG(500)OVA	1459 ± 189.4		−7.0 ± 0.5	74 ± 54
1 μm PEG(5k)OVA	1238 ± 23.4		−9.6 ± 0.4	42 ± 33

*OVA loading for each particle type was determined prior to dosing. Values represent average of 4–12 batches.